Quaternary Science Reviews 37 (2012) 92–104

Contents lists available at SciVerse ScienceDirect

Quaternary Science Reviews

journal homepage: www.elsevier.com/locate/quascirev

A ~43-ka record of paleoenvironmental change in the Central American lowlands inferred from stable isotopes of lacustrine ostracods

Jaime Escobar [a,b,c,*], David A. Hodell [d], Mark Brenner [e], Jason H. Curtis [e], Adrian Gilli [f], Andreas D. Mueller [f], Flavio S. Anselmetti [g], Daniel Ariztegui [h], Dustin A. Grzesik [d], Liseth Pérez [i], Antje Schwalb [i], Thomas P. Guilderson [j,k]

[a] Departamento de Ciencias Biológicas y Ambientales, Universidad de Bogota Jorge Tadeo Lozano, Colombia
[b] Center for Tropical Paleoecology and Archaeology (CTPA), Smithsonian Tropical Research Institute (STRI), Panama
[c] School of Natural Resources and Environment, and Land Use and Environmental Change Institute (LUECI), University of Florida, Gainesville, FL 32611, USA
[d] Godwin Laboratory for Palaeoclimate Research, Department of Earth Sciences, University of Cambridge, Downing Street, Cambridge CB2 3EQ, UK
[e] Department of Geological Sciences, and Land Use and Environmental Change Institute (LUECI), University of Florida, Gainesville, FL 32611, USA
[f] Geological Institute, ETH Zurich, 8092 Zurich, Switzerland
[g] Eawag, (Swiss Federal Institute of Aquatic Science & Technology), Ueberlandstrasse 133, P.O. Box 611, 8600 Duebendorf, Switzerland
[h] Section of Earth Sciences, University of Geneva, 1205 Geneva, Switzerland
[i] Institut für Umweltgeologie, Technische Universität Braunschweig, Langer Kamp 19c, 38106 Braunschweig, Germany
[j] Center for Accelerator Mass Spectrometry, Lawrence Livermore National Laboratory, Livermore, CA 94550, USA
[k] Institute of Marine Sciences, University of California, Santa Cruz, CA 95064, USA

ARTICLE INFO

Article history:
Received 1 October 2011
Received in revised form
17 January 2012
Accepted 20 January 2012
Available online 16 February 2012

Keywords:
Oxygen isotopes
Carbon isotopes
Lake sediments
Neotropics
Paleoclimatology
Last glacial
Last deglaciation

ABSTRACT

We present a continuous ostracod isotope ($\delta^{18}O$ and $\delta^{13}C$) record from Lake Petén Itzá, Petén, Guatemala, in the northern, lowland Neotropics that spans the last ~43 cal ka BP. Variations in oxygen and carbon isotopes closely follow lithologic variations, which consist of alternating gypsum and clay deposits that were deposited under relatively dry and wet climate, respectively. During the last glacial period, the greatest $\delta^{18}O$ and $\delta^{13}C$ values coincide with gypsum deposited during lake lowstands under arid climate conditions that were correlated previously with North Atlantic Heinrich events. In contrast, interstadials and the entirety of the Last Glacial Maximum (~24–19 cal ka BP) are marked by clay deposition and lower $\delta^{18}O$ and $\delta^{13}C$ values, reflecting higher lake levels and relatively moister climate.

Isotope results and pollen data, along with independently inferred past water levels, show the early deglacial period (~19–15 cal ka BP) was the time of greatest aridity and lowest lake stage of the past 43 ka. This period occurred during Heinrich Stadial 1 (HS 1), when an extensive tropical megadrought has been postulated (Stager et al., 2011). Heinrich Stadial 1 is represented by two episodes of gypsum precipitation and high $\delta^{18}O$ and $\delta^{13}C$ values in Petén Itzá, interrupted by an intervening period of lower $\delta^{18}O$ and $\delta^{13}C$ and clay deposition centered on ~17 cal ka BP. The two periods of inferred maximum cold and/or arid conditions at ~17.5 and 16.1 cal ka BP coincide approximately with two pulses of ice-rafted debris (IRD) recorded off southern Portugal (Bard et al., 2000). At ~15 cal ka BP, coinciding with the start of the Bolling-Allerod period, $\delta^{18}O$ and $\delta^{13}C$ decrease and gypsum precipitation ceases, indicating a transition to warmer and/or wetter conditions. Gypsum precipitation resumed while $\delta^{18}O$ and $\delta^{13}C$ increased at the start of the Younger Dryas at 13.1 cal ka BP and continued until 10.4 cal ka BP, near the onset of the Holocene.

Precipitation changes during the last glacial period in the northern hemisphere Neotropics were closely linked with freshwater forcing to the high-latitude North Atlantic, and sensitive to changes in the location of meltwater input. Climate was coldest/driest when meltwater directly entered the high-latitude North Atlantic, permitting sea ice expansion and weakening of Atlantic Meridional Overturning Circulation (AMOC), which resulted in a more southerly position of the Intertropical Convergence Zone (ITCZ). Upon deglaciation, when meltwater was directed to the Gulf of Mexico, at ~17 ka and

* Corresponding author. Departamento de Ciencias Biológicas y Ambientales, Universidad de Bogotá Jorge Tadeo Lozano, Bogota, Colombia. Tel.: +571 2427030x1538; fax: +571 2826197.
E-mail address: jaimeh.escobarj@utadeo.edu.co (J. Escobar).

0277-3791/$ – see front matter
doi:10.1016/j.quascirev.2012.01.020

during the Bolling-Allerod period (15–13 ka), precipitation increased in the northern hemisphere Neotropics as North Atlantic sea ice retreated and the ITCZ shifted northward. Results from Lake Petén Itzá offer some support for the meltwater routing hypothesis of Clark et al. (2001).

1. Introduction

There are few well-dated, high-resolution records of continental climate change in the Neotropics during the last glacial period. The best regional record for the late Pleistocene comes from the marine Cariaco Basin, north of Venezuela (Hughen et al., 1996; Peterson et al., 2000; Lea et al., 2003). A handful of lacustrine records in Central America have been reported, including La Chonta Bog, Costa Rica (Hooghiemstra et al., 1992; Islebe et al., 1995), Lake La Yeguada, Panama (Piperno et al., 1990; Bush et al., 1992), and Lake Quexil, Guatemala (Deevey et al., 1983; Leyden et al., 1993).

In 2006, a complete 85-ka record was drilled in Lake Petén Itzá, Guatemala, as part of a project sponsored by the International Continental Drilling Program (ICDP). Hodell et al. (2008) and Mueller et al. (2010) reported on the lithology and sedimentology of long sediment cores from this lake. They interpreted the paleoclimate history on the basis of alternating bands of clay and gypsum during the last glacial and deglacial periods, which were thought to reflect wet and dry climate conditions, respectively. Beginning ~48 ka BP, climate varied between wetter conditions during interstadials and drier conditions during stadials. Arid periods were correlated to Greenland stadials and particularly Heinrich events, when the Atlantic Intertropical Convergence Zone (ITCZ) was located far to the south (Colinvaux et al., 1996; Baker et al., 2001; Bush et al., 2004). Moister conditions prevailed during interstadials and the Last Glacial Maximum (LGM).

Here we present a continuous, high-resolution (~decadal), stable isotope record ($\delta^{18}O$ and $\delta^{13}C$) from Lake Petén Itzá that spans the last ~43 ka. Interpretation of the oxygen isotope record in the context of lithologic change permits a detailed reconstruction of climate history for the last glacial period in the lowlands of northern Central America. Furthermore, the isotope record elucidates climate teleconnections between the northern Neotropical lowlands and the wider Caribbean, Gulf of Mexico, and North Atlantic basins.

2. Study site

Lake Petén Itzá (~16°55′ N, 89°50′ W) is located in the Petén Lake District, in lowland northern Guatemala (Fig. 1). It has a surface area of ~100 km^2 and a maximum water depth >160 m (Anselmetti et al., 2006). Lake Petén Itzá receives hydrologic inputs from direct rainfall, runoff, and subsurface groundwater. It lacks surface outlets and although some seepage loss may occur, it is effectively a closed-basin lake (Hodell et al., 2008). Lake Petén Itzá's water is dilute (11.22 meq/l) and is dominated by calcium and magnesium cations and bicarbonate and sulfate anions (Hillesheim et al., 2005). Lakewater pH is high (~8.0) and at present the lake is saturated with calcium carbonate, which precipitates and accumulates in shallow zones of the lake (Hodell et al., 2008; Mueller et al., 2009). Today, lakewater $\delta^{18}O$ averages 2.6‰ (Hillesheim et al., 2005), greater than the mean value for regional surface and groundwater (−3.0‰) (Lachniet and Patterson, 2009), reflecting the importance of evaporation in the lake's water budget.

Lake Petén Itzá is situated in a climatically sensitive region. Although the ITCZ does not reach latitudes higher than ~15°N, the

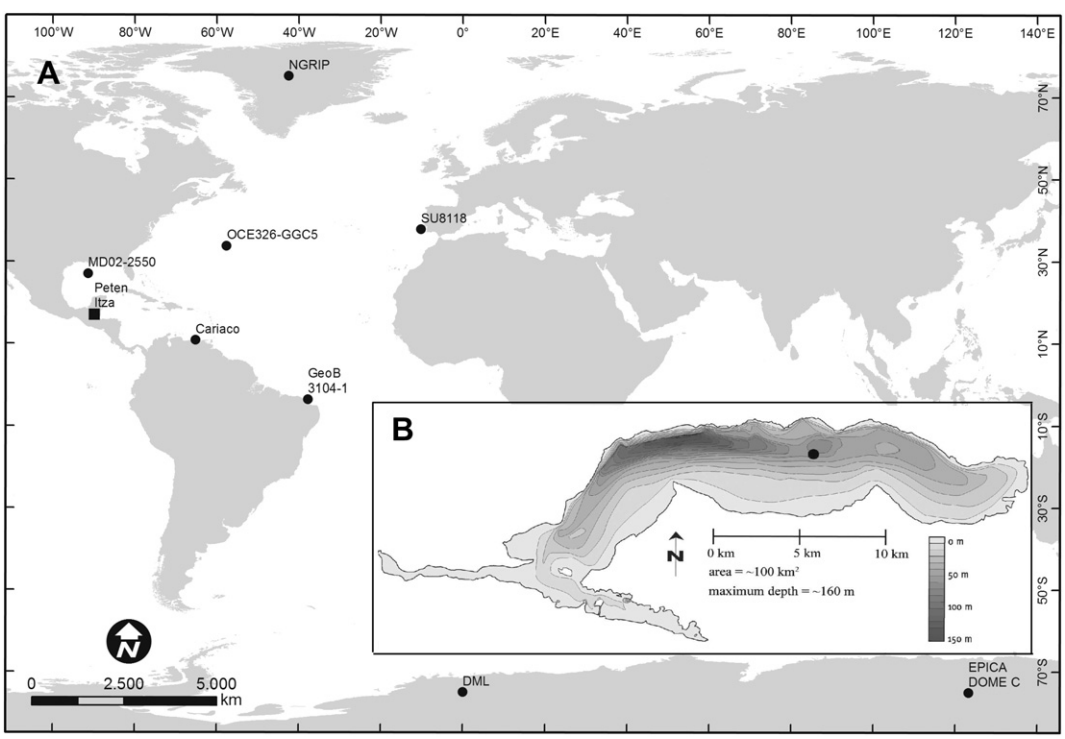

Fig. 1. (A) Map showing the locations of Lake Petén Itzá, northern Guatemala, and paleoclimate reconstruction sites discussed in this paper. (B) Bathymetric map of Lake Petén Itzá showing the location of drilling site PI-6.

amount of rainfall in the area is associated with the seasonal migration of the ITCZ and less spatially oriented tropical convective activity (Hastenrath, 1984; Poveda et al., 2006; Hodell et al., 2008). The rainy season, associated with the northward migration of the ITCZ, occurs between June and December, when easterly trade winds transport moisture from the Atlantic into the Caribbean Sea and the Yucatán Peninsula. The pronounced dry season occurs during northern hemisphere winter, January through May, when the ITCZ moves southward. During the dry season, light winter precipitation is sometimes brought to the Yucatán Peninsula by northerly winds from polar air masses (Portig, 1965; Hastenrath, 1984, 2002; Poveda et al., 2006).

3. Field and laboratory methods

Between 3 February and 11 March 2006, we collected sediment cores from seven sites in Lake Petén Itzá under the auspices of the ICDP (Hodell et al., 2006, 2008). Sediment cores from a water depth of 71 m at Site PI-6 (Fig. 1) provide a continuous stratigraphic sequence to ~75.9 m composite depth (mcd), which represents ~85 cal ka of sediment accumulation (Hodell et al., 2008).

Samples from 1-cm core sections from Site PI-6 were disaggregated with 3% H_2O_2 solution to obtain ostracod valves (*Limnocythere opesta*, Brehm, 1939) for stable isotope analysis. Samples were washed through a 63-μm sieve and material was collected on filter paper and dried at 50 °C. When dry, the material was transferred to glass scintillation vials. Adult specimens of *L. opesta* were picked from the sieved, >212-μm fraction in each 1-cm sample using a binocular microscope. Prior to isotopic analysis, ostracod specimens were cleaned using 15% H_2O_2 to remove organic material, and rinsed in methanol before drying. Ostracod valves were checked for impurities and cleaned again if necessary. Approximately 12–20 individual ostracod valves, weighing a total of ~20–60 μg, were used for all samples. Multiple ostracod specimens were measured from each stratigraphic level to reduce the variance associated with analyzing single, short-lived individuals (Heaton et al., 1995; Escobar et al., 2010). Ostracod valves were loaded into glass vials and CO_2 was evolved from shells with a single-aliquot acid digestion in a Kiel III carbonate preparation device attached to a Finnigan-MAT 252 isotope ratio mass spectrometer at the University of Florida. Summary statistics on the standard NBS-19, $n = 336$, yielded a mean and standard deviation of -2.20 ± 0.07 for $\delta^{18}O$ and 1.95 ± 0.04 for $\delta^{13}C$.

The record for the last glacial period spans 43 to 10 cal ka BP and was produced by measuring stable isotopes of calcite composed of monospecific specimens of the ostracod *L. opesta*. This species is present and generally abundant throughout the glacial and Late-glacial periods (Pérez et al., 2011). Living specimens of *L. opesta* are today found to a maximum water depth of 40 m, though valves are encountered a greater depths, and *L. opesta* shells dominate surface sediment ostracod assemblages in water depths from the littoral zone to 40–50 m, i.e. to the base of the thermocline (Pérez et al., 2010). The Pleistocene/Holocene transition and Holocene oxygen isotope record was compiled using published data on three ostracod species from different coring sites in Lake Petén Itzá. The record for the Pleistocene/Holocene transition and early Holocene consists of isotope values measured on *Pseudocandona* sp., Kaufmann, 1900, *Cytheridella ilosvayi*, Daday, 1905 (Curtis et al., 1998), and *Limnocythere* sp., Brady, 1886 (Hillesheim et al., 2005).

Oxygen isotopes of calcite carapaces from modern individuals of these species from different water depths in Lake Petén Itzá indicate the ostracods do not precipitate calcite in oxygen isotopic equilibrium with ambient water. This is attributed to species-specific "vital effects" (Fig. 2). Oxygen isotopes of other species were normalized to those of *L. opesta*, which itself precipitates

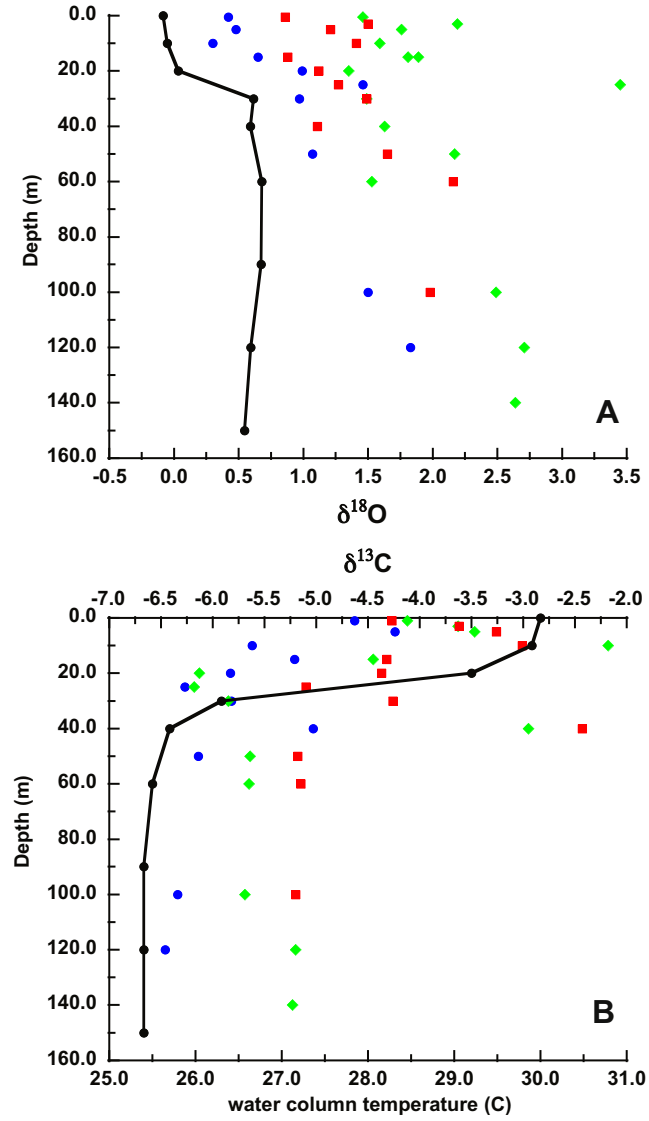

Fig. 2. (A) Modern $\delta^{18}O$ values on *Limnocythere opesta* (blue circles), *Pseudocandona* sp. (green diamonds), and *Cytheridella ilosvayi* (orange squares) at different depths. Black line represents the $\delta^{18}O$ of equilibrium calcite calculated using temperature and water $\delta^{18}O$. (B) Modern $\delta^{13}C$ values of *Limnocythere opesta* (blue circles), *Pseudocandona* sp. (green diamonds), and *Cytheridella ilosvayi* (orange squares) at different depths. Black line represents water temperatures at different depths. (For interpretation of the references to colour in this figure legend, the reader is referred to the web version of this article.)

oxygen isotopes at an offset from equilibrium of about 0.5‰. On average, isotope measures on *Pseudocandona* sp. exceed those of *L. opesta* by 1.04‰, and mean values for *C. ilosvayi* are greater than those of *L. opesta* by 0.54‰. No attempt was made to normalize carbon isotopes because of the different depth habitats of ostracod species in both the water and sediment column.

4. Interpretation of proxies

4.1. Oxygen isotopes

In closed-basin Lake Petén Itzá, the relative amount of evaporation to precipitation (E/P) is the principal control on lakewater chemistry, including oxygen isotopes. Periods of high E/P are expected to yield lower lake levels, greater concentrations of

dissolved solids, and higher water-column $\delta^{18}O$. Conversely, during episodes of low E/P, lake stage is higher, lake water is more dilute, and $\delta^{18}O$ of water is lower.

In addition to changing E/P, the $\delta^{18}O$ of lake water is also affected by the $\delta^{18}O$ of rainfall that, in part, depends on the isotope composition of the moisture source, i.e., seawater. It is also influenced by the extent of moisture depletion (i.e., rainout) in the air mass as it is transported from the source area to the rainfall region. There is progressive depletion of $H_2^{18}O$ with increasing latitude, altitude, distance from the coast, and rainfall amount. Lastly, the $\delta^{18}O$ of rainfall is controlled by the relative humidity and temperature of the atmosphere from the time water evaporates from the ocean to the moment a raindrop hits the ground (Dansgaard, 1964; Darling et al., 2006; Leng et al., 2006).

Lakewater $\delta^{18}O$ and water temperature largely determine the $\delta^{18}O$ in the calcium carbonate of shell-forming aquatic organisms such as ostracods and gastropods. Colder temperatures yield greater $\delta^{18}O$ values in precipitated carbonate, whereas warmer temperatures produce lower $\delta^{18}O$ values. A switch from higher to lower $\delta^{18}O$ values in ostracod shells in a sediment sequence may reflect: 1) a change in precipitation source and/or isotopic composition, and/or 2) a change from colder and/or drier, to warmer and/or wetter conditions. Conversely, a change from lower to higher $\delta^{18}O$ could reflect: 1) a change in precipitation source and/or isotopic composition, and/or 2) a change to colder and/or drier conditions.

4.2. Carbon isotopes

The $\delta^{13}C$ of lakewater dissolved inorganic carbon (DIC) is influenced by a host of factors including: (1) the carbon isotope composition of input waters; (2) CO_2 exchange between the lake and the atmosphere; (3) photosynthesis-respiration; and (4) processes that occur in the mud (organic carbon oxidation, sulfate reduction, and methanogenesis) (Oana and Deevey, 1960). In thermally or chemically stratified lakes, a strong $\delta^{13}C$ gradient often develops between the epilimnion and hypolimnion as a result of photosynthetic biological pumping of ^{12}C from surface to deep water. Benthic ostracods record the $\delta^{13}C$ of overlying lakewater DIC and are also affected by pore water $\delta^{13}C$, which can be depleted or enriched relative to lake water owing to the oxidation of sediment organic matter or methanogenesis, respectively. Methanogenesis is suppressed in Lake Petén Itzá because of abundant dissolved sulfate in the water column and pore waters, the latter owing to gypsum in the sediments.

4.3. Lithology

Petén Itzá's sediments consist of a mixture of inorganic and organic matter of autochthonous and allochthonous origin. Sediment organic matter produced within the lake comes from phytoplankton, higher plants, zooplankton, benthic organisms, and their fecal matter. Autochthonous inorganic matter comes in the form of calcite, dolomite, and gypsum, precipitated from the water column. External sources of organic matter include leaves, twigs, and pollen grains, as well as organic matter in eroded surface soils. Clay, principally montmorillonite, constitutes the major detrital input, but carbonates from the watershed may also reach the lake in detrital form. Gypsum crystals are precipitated when lake or pore water exceeds saturation, which occurs when evaporation rates are high and rainfall is relatively low. The presence of gypsum in sediments therefore indicates dry periods in the past, when the volume of Lake Petén Itzá was reduced (Hillesheim et al., 2005; Hodell et al., 2008; Mueller et al., 2010). In contrast, deposition of clay indicates wet periods and higher lake levels, when runoff and the influx of detrital material were enhanced. Variations in sediment magnetic susceptibility reflect changes in sediment lithology, with high values associated with clay-rich horizons and low values associated with gypsum deposits, thereby representing wet and dry climate episodes, respectively (Hodell et al., 2008).

5. Core chronology

All radiocarbon analyses were made on terrestrial macrofossils, thereby avoiding potential dating errors associated with autochthonous organic matter from this hard-water lake (Deevey and Stuiver, 1964). Samples were chemically pretreated (acid-base-acid). Radiocarbon ages include a background subtraction using an appropriate ^{14}C-free matrix and $\delta^{13}C$ correction and are reported according to the convention set forth in Stuiver and Polach (1977).

The initial age/depth model for core PI-6 was developed using 18 AMS ^{14}C dates on terrestrial remains from cores taken at sites PI-6 and PI-3 (Hodell et al., 2008; Mueller et al., 2010). Dates from core PI-3 were projected onto core PI-6 by correlating the magnetic susceptibility records from the two sequences. New dates on terrestrial remains from cores taken at drill sites PI-2 and PI-6 enabled refinement of the age/depth model presented in Hodell et al. (2008) (Supplementary material). Dates from the PI-2 and PI-3 cores were again projected onto core PI-6 by detailed correlation of the magnetic susceptibility records (Fig. 3) as magnetic susceptibility variations reflect gypsum/clay variations that are thought to be synchronous across the basin. We assume no error in the projection of the individual stratigraphies onto the common depth scale. A total of 64 dates were obtained and span the last 43 ka of the record. In general, replicate analyses overlapped at 1-sigma analytical uncertainty. Such replicate samples were averaged and then calibrated. Clusters of samples producing reversals at ~40, ~30, and ~8 ka years BP were not included in the age/depth model (Supplementary material). Criteria for sample rejection were based on out-of-sequence dates, assuming that anomalously old ages in the sequence reflected reworking in the watershed of the dated material, high standard deviation values (due to very small sample size) and potential abrupt sedimentation rate changes. The new core chronology is based on 36 age/depth points generated from 44 ^{14}C dates (Table 1, Fig. 4). The new age model includes 12 dates for the deglaciation, whereas the earlier age model (Hodell et al., 2008) only included six dates for the period ~19–10 cal ka BP. Furthermore, the new age model excludes two dates included in the earlier model (Hodell et al., 2008), 20.3 mcd (~16.5 cal ka BP) and 17.12 mcd (~14.1 cal ka BP), as new dates from Sites PI-2 and PI-6 demonstrate that these two samples were out of sequence. New dates on nearby depth intervals at 19.76 and 17.55 mcd have dates of ~18.1 and ~16.6 cal ka BP, respectively.

In contrast to the chronology presented in Mueller et al. (2010), which utilized the Fairbanks et al. (2005) calibration, we calibrated the ^{14}C ages using the IntCal-09 ^{14}C-calendar calibration data (Reimer et al., 2009). Although both calibration approaches are based on surface marine samples (planktonic foraminifera and hermatypic reef-building corals) and assume constant surface ocean reservoir ages, a nearly continuous record derived from the updated Cariaco on Hulu Cave timescale (Reimer et al., 2009) and a rigorous comparison with alternative near calibration-data-sets, show that the IntCal-09 deglacial and older sequence is superior to that of Fairbanks et al. (2005). The tree-ring calibration sequence to ~12.5 ka is 'common' to the Fairbanks et al. (2005) calibration.

Radiocarbon dates were calibrated using the program Oxcal-Intcal09 (Bronk-Ramsey, 2001, 2008; Reimer et al., 2009). The age model is based on a piecewise linear interpolation that includes the underlying non-Gaussian uncertainty in the calibrated age probability distribution. Confidence intervals (95%) were estimated via

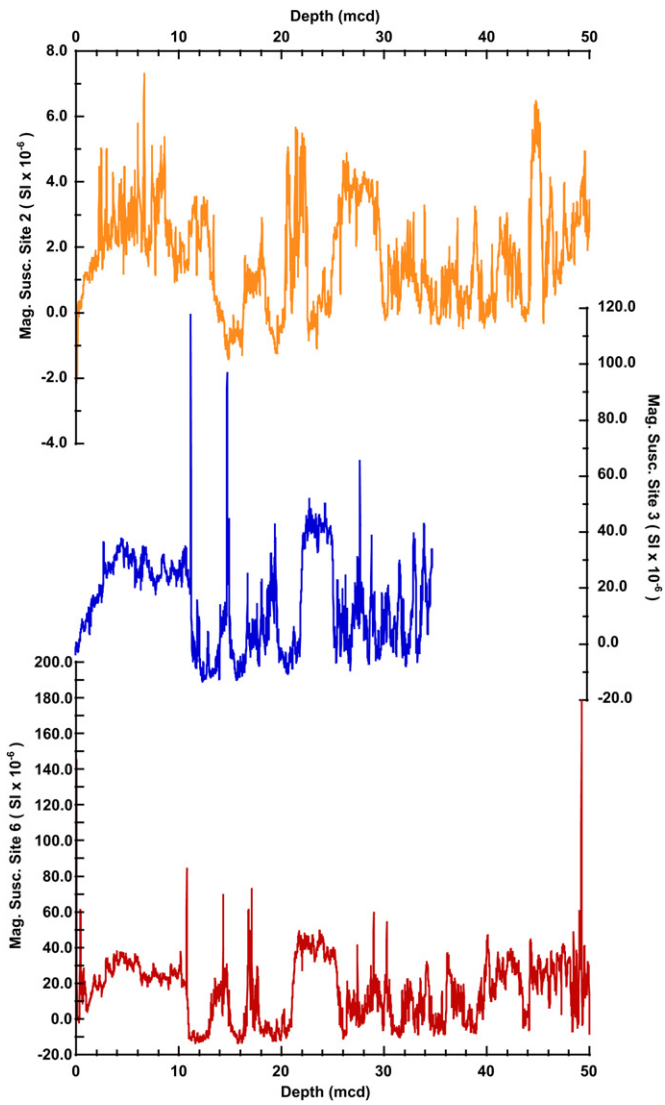

Fig. 3. Spliced magnetic susceptibility records from Sites PI-2 (yellow), PI-3 (blue), and PI-6 (red) on their own depth scale. (For interpretation of the references to colour in this figure legend, the reader is referred to the web version of this article.)

1000 iterations of the piece-wise linear age model using 'classical' age modeling (CLAM) (Blaauw, 2010). Although the age model is constructed from ^{14}C dates from three cores, the isotope data are from a single core. Thus stratigraphic consistency in the isotope data is maintained regardless of the uncertainty in the age model.

6. Results

During Marine Isotope Stage 3 (MIS3) and the LGM, oxygen isotope values displayed a mean of ~ +5.0‰, and generally ranged from about +4.0–6.0‰ (Fig. 5). The most positive $\delta^{18}O$ values (>7.0‰) are associated with HS 1 in the early deglacial, with peaks at ~17.5 and ~16.1 cal ka BP (Fig. 5). Thereafter, $\delta^{18}O$ values decrease to 4.5‰ during the period 15.3–13.1 cal ka BP, roughly coinciding with the Bolling/Allerod period (14.7–12.9 cal ka BP, Rasmussen et al., 2006) and increase to 5.5‰ again during the interval 13.1–11.5 cal ka BP, approximately the span of the Younger Dryas (12.9–11.7 cal ka BP, Rasmussen et al., 2006) (Fig. 5). Oxygen isotopes decreased to ~3.5‰ in the early Holocene. A further $\delta^{18}O$ decrease of about ~2‰ occurred during the early to middle Holocene (Curtis et al., 1998).

Carbon isotopes show large variations, from values as low as −11‰, to as high as +1‰ (Fig. 5). High $\delta^{13}C$ values occurred during each of the Heinrich events, with the greatest values (~0.0‰) occurring in the deglaciation, between ~19.0 and ~15.3 cal ka, during HS 1. From ~15.3 to ~13.1 cal ka, spanning much of the Bolling/Allerod period, $\delta^{13}C$ values decrease to −7.5‰ (Fig. 5). Carbon isotopes increase to near 0‰ again from ~13.1 to ~10.5 cal ka during the Younger Dryas and Preboreal Periods (Fig. 5). This is followed by a sharp decrease in $\delta^{13}C$ during the Holocene (Fig. 5).

7. Discussion

Variations in ostracod $\delta^{18}O$ and $\delta^{13}C$ are tightly coupled with changes in sediment lithology, such that high isotopic values correspond to gypsum-rich layers and low values to clay-rich deposits. The simplest interpretation of these variables is they are responding to fluctuating climate conditions (evaporation/precipitation) and attendant changes in lake stage and volume. During periods of arid climate (high E/P), the lake volume is reduced, $\delta^{18}O$ increases, and gypsum saturation is exceeded. We speculate that variations in ostracod $\delta^{13}C$ are controlled by the position of Site PI-6 relative to the thermocline and secondarily by organic carbon flux to the sediment. Higher $\delta^{13}C$ is associated with lower lake level when the site is within the oxygenated epilimnion. Lower organic carbon (C_{org}) content in the gypsum sands deposited during arid intervals also results in less steep $\delta^{13}C$ pore water gradients between the sediment surface and depth. The ostracods thus record higher $\delta^{13}C$ values. During wetter climate conditions, $\delta^{18}O$ decreases and sediment composition is dominated by clay. During lake high stands, $\delta^{13}C$ records low-oxygen hypolimnetic DIC that is depleted in ^{13}C due to organic matter oxidation both in the water column and sediment pore waters. We interpret the climate history for the past 43 cal ka BP on the basis of varying $\delta^{18}O$ and $\delta^{13}C$ of ostracod calcite and sediment composition.

7.1. MIS 3 (~43–24 cal ka BP)

Oxygen isotope values of *L. opesta* were fairly constant during late Marine Isotope Stage 3 (MIS3), averaging ~5.0‰, with maximum values of ~7.0‰. Oxygen and carbon isotopes show distinct peaks at 38, 31, and 24 cal ka BP, which coincide closely with the estimated timing of H4, H3 and H2 (Hemming, 2004). At these times, core lithology changed from clay to gypsum (Fig. 5), suggesting lake volume declined and concentrations of dissolved calcium sulfate exceeded saturation. The oxygen and carbon isotope records provide support for previous climate inferences based on lithologic variations (Hodell et al., 2008).

Modern *L. opesta* $\delta^{18}O$ values in samples to 100 m depth in Lake Petén Itzá range from ~0.0‰ to ~1.5‰. Thus, mean MIS3 values are >3.5‰ greater than $\delta^{18}O$ of modern *L. opesta*, and values during Heinrich events are ~5.5‰ greater than modern. If the high $\delta^{18}O$ values in late MIS3 were attributable solely to temperature, it would have required a mean temperature decrease of 14.0 °C, and a decrease of 22.0 °C during Heinrich events, relative to present. These highly improbable temperature changes indicate that a substantial part of the $\delta^{18}O$ signal must be due to changing $\delta^{18}O$ of lake water. Measurement of gypsum hydration water during the Lateglacial period at Site PI-6 indicates that $\delta^{18}O$ of lake water ranged from 5.5 to 7‰, which is 2.5–4‰ greater than today (Hodell et al., 2012).

Table 1
Age-depth points used to derive chronology shown in Fig. 3.

Accession #	Site	Depth in site mcd	Depth in site 6 mcd	Age 14C yr B.P.	± (1s)	Interpolated cal yrs BP		
						Minimum 95%	Maximum 95%	Best
144277	2	0.32	0.32	425	30	333	527	479
139341	2	4.88	4.00	1715	35	1541	1706	1625
128603	3	4.22	4.18	2140	40	1995	2321	2143
125903	6	8.08	8.08	3905	35	4260	4420	4343
125895	6	8.08	8.08	3920	35			
144270	2	11.14	8.68	4280	30	4821	4948	4850
128604	3	9.37	8.90	4590	40	5095	5377	5244
128614	3	9.37	8.90	4550	35			
139344	2	12.16	9.63	7455	35	8210	8353	8282
139417	2	12.16	9.63	7480	45			
139346	2	13.06	10.47	7835	30	8546	8699	8613
128605	3	11.32	10.69	8625	35	9547	9661	9601
128615	3	11.32	10.69	8675	35			
131226	6	10.86	10.86	9040	35	10182	10243	10213
128606	3	14.17	13.06	11210	35	12927	13257	13108
128611	6	13.35	13.35	11290	60	13075	13321	13187
128613	6	13.41	13.41	11380	140	12951	13561	13253
131224	6	13.87	13.87	11390	50	13144	13386	13264
139399	2	17.74	14.26	11880	35	13593	13871	13734
128612	6	14.49	14.49	12460	60	14138	15015	14565
144272	2	20.71	16.81	13095	40	15205	16464	15860
139400	2	21.91	17.55	13480	45	16353	16889	16640
139401	2	22.13	17.68	13505	45	16522	16852	16692
139418	2	22.13	17.68	13560	45			
144268	2	23.93	19.76	14810	45	17850	18457	18129
144280	2	23.93	19.76	14850	45			
139402	2	25.74	21.20	15355	50	18495	18759	18610
125898	6	23.64	23.64	17650	240	20367	21541	20966
144274	2	28.62	24.63	19740	70	23290	23890	23590
125899	6	25.73	25.73	19990	180	23406	24382	23895
144269	2	31.75	27.85	21940	80	25995	26811	26395
128607	3	28.09	29.16	23210	90	27719	28277	27989
128616	3	28.09	29.16	23040	90			
139403	2	34.43	30.64	25540	160	29719	30874	30386
128608	3	30.09	31.77	26560	130	30940	31294	31119
139414	6	31.86	31.86	26660	240	30910	31454	31161
139415	6	31.89	31.89	26820	260	30967	31542	31239
125901	6	33.83	33.83	29120	170	33264	34261	33764
125905	6	33.83	33.83	29010	170			
144278	6	35.14	35.14	31230	260	35061	36469	35759
128609	3	33.42	37.82	32820	260	36664	38481	37438
139405	2	44.83	40.12	34380	450	38507	40707	39499
126528	6	42.76	42.76	35900	1200	38717	42853	40858
126527	6	45.31	45.31	38100	1100	41306	44368	42793

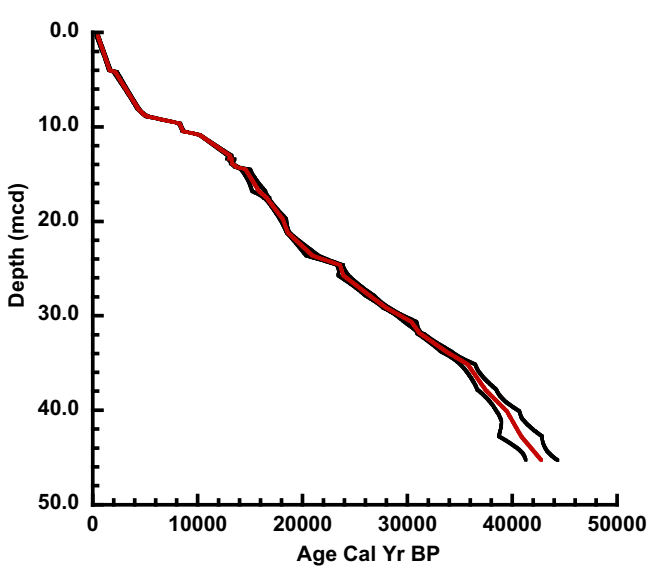

Fig. 4. Calibrated radiocarbon dates versus mcd. Black lines represent a 95% confidence interval range.

7.2. Last Glacial Maximum (~24–19 cal ka BP)

Ostracods are sparse during the LGM chronozone (~24–19 cal ka BP), but measured $\delta^{18}O$ values are ~5‰, about equal to the mean late MIS3 $\delta^{18}O$ value (Fig. 5). Contrary to interpretations from earlier studies (Leyden et al., 1993, 1994), the LGM was not especially dry in Petén. Clay-rich sediments accumulated rapidly between ~24 and 19 cal ka BP (Mueller et al., 2010), indicating relatively high lake levels and relatively wet climate conditions (Hodell et al., 2008). Low $\delta^{13}C$ is consistent with high lake levels, indicating the sediment–water interface at Site PI-6 was below the thermocline. Pollen analysis indicates an LGM assemblage consisting of a scrub oak or montane pine-oak forest, consistent with moist conditions and air temperatures at least 4.0–6.0 °C cooler than today (Bush et al., 2009), similar to temperatures in the low-latitude western Atlantic (Guilderson et al., 2001).

A wetter LGM in lowland Central America might be explained by greater summer precipitation, caused by a more northerly position of the Atlantic ITCZ. McManus et al. (2004) inferred that AMOC strength in the LGM was similar to the strength during the Bolling-Allerod period, a time for which there is evidence of a northerly

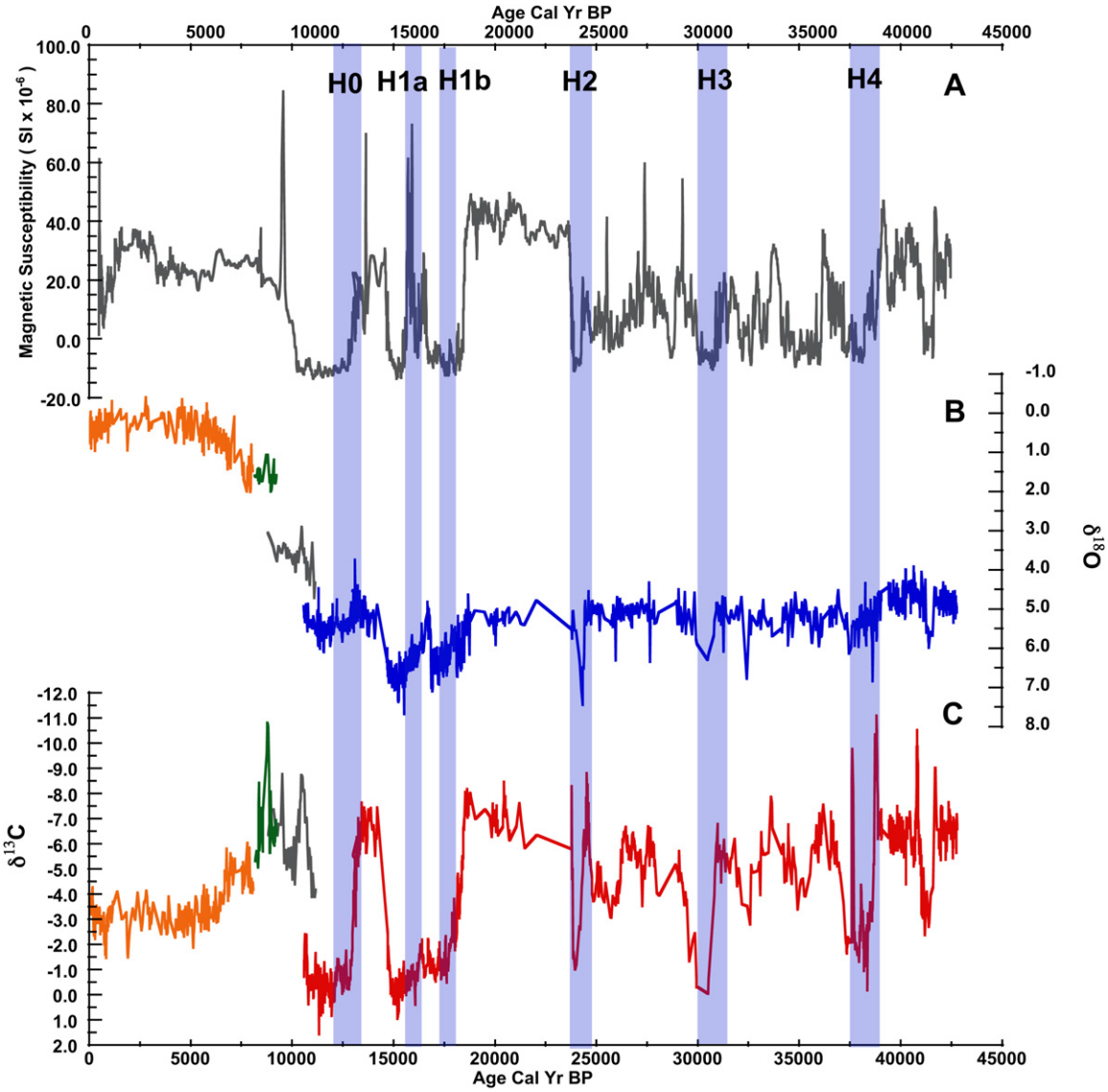

Fig. 5. (A) Magnetic susceptibility of Lake Petén Itzá Site PI-6. (B) Oxygen isotope data for Lake Petén Itzá for the last 43.0 cal ka years. $\delta^{18}O$ data indicated by a blue line (*Limnocythere opesta*) are from PI-6. $\delta^{18}O$ data indicated by a grey line (*Limnocythere* sp.) are from Lake Petén Itzá core 11A (Hillesheim et al., 2005). $\delta^{18}O$ data indicated by an orange line (*Cytheridella ilosvayi*) and a green line (*Pseudocandona* sp.) are from Lake Petén Itzá core 6-VII-93 (Curtis et al., 1998). (C) Carbon isotope data for Lake Petén Itzá for the last 43.0 cal ka years. $\delta^{13}C$ data indicated by a red line (*Limnocythere opesta*) are from PI-6. $\delta^{13}C$ data indicated by a grey line (*Limnocythere* sp.) are from Lake Petén Itzá core 11A (Hillesheim et al., 2005). $\delta^{13}C$ data indicated by an orange line (*Cytheridella ilosvayi*) and a green line (*Pseudocandona* sp.) are from Lake Petén Itzá core 6-VII-93 (Curtis et al., 1998). The thickest gypsum deposits, marked by low magnetic susceptibility, are highlighted by blue shading and correlate with increasing $\delta^{18}O$ and $\delta^{13}O$ values and Heinrich events. (For interpretation of the references to colour in this figure legend, the reader is referred to the web version of this article.)

ITCZ position (Peterson et al., 2000). Alternatively, greater winter precipitation from increased intensity and frequency from the north may also account for wetter LGM conditions in Petén (Hodell et al., 2008). During the LGM, the Laurentide Ice Sheet modified atmospheric circulation over North America. Wetter climate in the American southwest and western Mexico during the LGM has been explained by the split of the jet stream into a dry north and wet south branch, due to the presence of the Laurentide Ice sheet (Kutzbach and Guetter, 1986; Bradbury, 1997). Early climate models showed that a split westerly jet stream could bring precipitation to at least 20° N (Kutzbach and Guetter, 1986). More recent climate models suggest that the northern and southern branches were located farther south and that splitting of the westerly jet occurred only during winter months (Bromwich et al., 2004; Kim et al., 2008). The model of Kim et al. (2008) shows that although precipitation apparently increased in winter, it decreased during summer. In their model, average annual climate conditions during the LGM were drier than present. Wet conditions during the LGM in the Yucatan Peninsula might have also been a consequence of the mobile polar high (Leroux, 1993). Polar outbreaks of air from the north Pacific could have reached lower latitudes and migrated westward, and low-pressure cells could have moved moister eastern tropical Pacific air to the northeast, providing winter precipitation for the Yucatan Peninsula (Leroux, 1993).

7.3. Heinrich Stadial 1 (~19–15 cal ka BP)

The Petén Itzá isotope results, together with pollen data and independent reconstructions of past water levels, show that the early deglacial period was the time of lowest lake stage, maximum

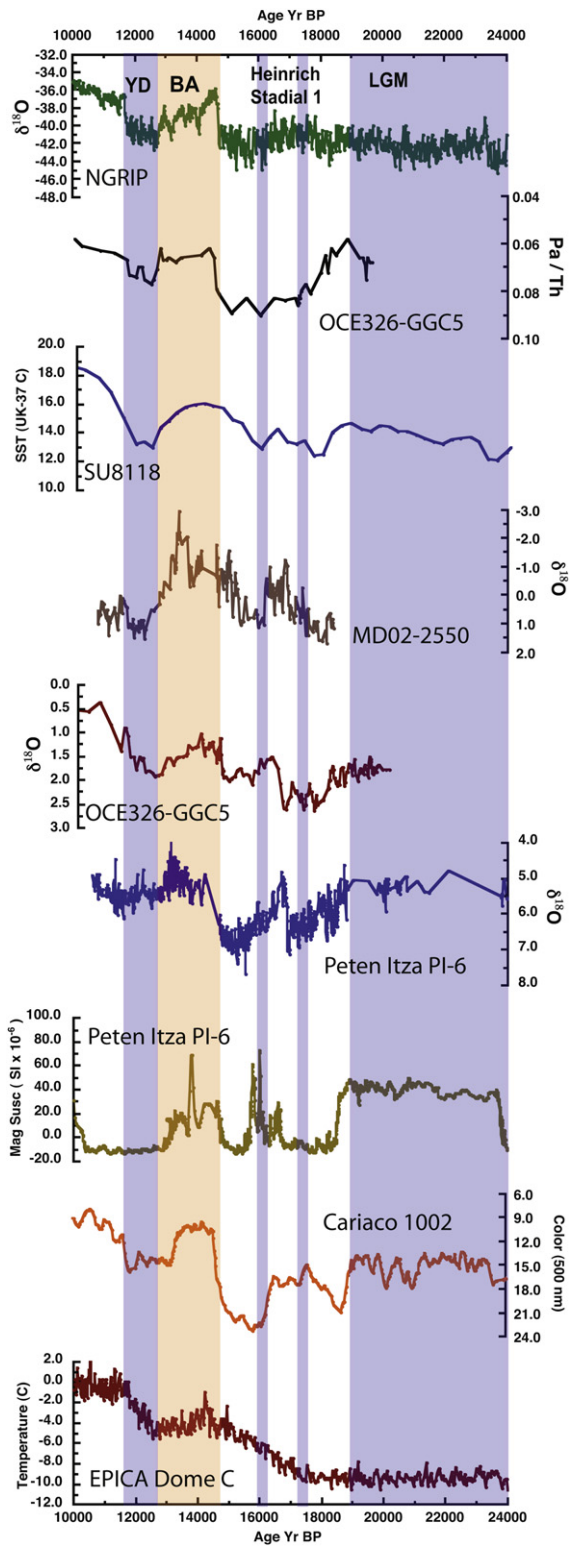

Fig. 6. (A) $\delta^{18}O$ of the North Greenland Ice Core Project members, 2004, (B) $^{231}Pa/^{230}Th$ from the Bermuda Rise core OCE326-GGC5 (McManus et al., 2004) (C) sea surface temperatures derived from alkenones in core SU8118 from the subtropical NE Atlantic (Bard et al., 2000), (D) $\delta^{18}O$ from the Orca Basin, Gulf of Mexico, core MD02-2550 (Williams et al., 2010), (E) $\delta^{18}O$ from the Bermuda Rise core OCE326-GGC5 (Carlson et al., 2008), (F) $\delta^{18}O$ of Lake Petén Itzá Site PI-6, (G) Magnetic susceptibility of Lake Petén Itzá Site PI-6 (Hodell et al., 2008) (H) color reflectance from the Cariaco Basin ODP site 1002 (Peterson et al., 2000) and (I) temperature reconstruction from Antarctica EPICA Dome C (Jouzel et al., 2007). Each record is plotted on its own, independent time scale. The light blue and red bands represents the Last Glacial Maximum (24.0–19.0 cal ka BP) corresponding approximately to the working definition of the LGM chronozone adopted by Mix et al. (2001), the pulses of ice-rafted debris (IRD) recorded off southern Portugal at ~17.5 (H1b) and ~16.1 (H1a) cal ka BP as define by Bard et al. (2000) and the Bolling-Allerod and Younger Dryas periods based on Greenland Ice Core Chronology 2005 (GICC05) (Rasmussen et al., 2006). (For interpretation of the references to colour in this figure legend, the reader is referred to the web version of this article.)

aridity, and the coldest period of the last 45 ka of the record (Bush et al., 2009; Hodell et al., 2012). Aridity in HS1 appears to have been both longer in duration and more severe than Heinrich events of MIS 3. Three stacked paleoshorelines were identified in seismic profiles at ~68 m, ~64 m and ~56 m, which correspond with three lowstands during the deglacial period between 18 and 11 ka (Mueller et al., 2010). Given that the modern water depth at PI-6 is 71 m and ~11 m of sediment accumulated in the Holocene, the minimum water depth at the site during the deglacial period could have been as shallow as ~10 m. At such times, the water column above Site PI-6 was likely well mixed and oxygenated, as suggested by the high deglacial $\delta^{13}C$ values (Fig. 5).

The driest climate of the last 45 ka, inferred from the Petén Itzá record, occurred during or about HS 1. Dry conditions in the northern hemisphere tropics during HS 1 have been attributed to a mean southerly position of the ITCZ because of meltwater input to the North Atlantic that reduced AMOC (Ganopolski and Rahmstorf, 2001; Knutti et al., 2004; Cheng et al., 2007; Liu et al., 2009). Stager et al. (2011) found HS1 was also a time of profound and widespread megadrought throughout the Afro-Asian tropics. They suggested the pattern of megadrought during HS1 could not be attributed solely to inter-hemispheric movement of the ITCZ because it included Afro-Asian regions in both hemispheres, i.e. north and south of the equator. Instead, the drought was likely related to cold tropical Atlantic sea surface temperatures (SSTs) and decreased moisture content in the ITCZ, regardless of its latitudinal position. Tropical North Atlantic SST also has an important influence on Caribbean and Central American summer rainfall variability (Hastenrath, 1978; Enfield, 1996; Enfield and Alfaro, 1999; Giannini et al., 2000; Taylor et al., 2002; Spencer et al., 2004; Wang et al., 2006), which may partly explain the generally arid condition during HS 1.

The entirety of HS1, however, was not arid. The Lake Petén Itzá $\delta^{18}O$ record shows two cold, dry periods punctuated by a relatively warmer, wetter period (Fig. 6). This climate pattern might be explained by two events of freshwater flux to the North Atlantic during HS1. Two pulses of ice-rafted debris (IRD) were recorded off southern Portugal, at ~17.5 (H1b) and ~16.1 (H1a) cal ka BP, with an intervening period of warmer surface water (Bard et al., 2000). The two IRD pulses may correspond to the cold, arid events in the Petén Itzá record, and the intervening period of warm sea surface water may correspond to a short-lived event beginning at ~17 ka in the Petén Itzá record, when clay was deposited and ostracod $\delta^{18}O$ decreased, indicating somewhat moister conditions. Other records from the Caribbean, Gulf of Mexico, and North Atlantic suggest that HS1 was interrupted by a similar event. In the Cariaco Basin, a distinct gray unit was deposited in the midst of HS1 and interpreted to represent increased rainfall and fluvial discharge (Yurco, 2010). On the Bermuda Rise, Carlson et al. (2008) showed an increase in temperature and a decrease in $\delta^{18}O$ of *Globorotalia inflata*, d'Orbigny, 1839 at 16.5 ka, punctuating an otherwise cold period during HS1 (Fig. 6).

At about the same time (17 ka), the $\delta^{18}O$ of the Orca Basin decreased below 0‰ (SMOW), indicating early meltwater input to the Gulf of Mexico (GOM), which preceded the main meltwater pulse during the Bolling-Allerod (14.7–12.7 ka) (Williams et al., 2010). Although meltwater input to the GOM can affect AMOC,

the response is about half that of direct input to the North Atlantic (Otto-Bliesner and Brady, 2010). More importantly, southward routing of meltwater has very little impact on North Atlantic sea ice extent (Roche et al., 2010). Modeling studies have shown a strong sensitivity of the position of the ITCZ to high-latitude sea ice (Chiang and Bitz, 2005) and the latitudinal temperature gradient (Rind and Rossow, 1984). We suggest the relatively warm, wet period at ~17 ka during HS1 may have been a consequence of brief rerouting of freshwater input from the North Atlantic to the GOM during the initial retreat of Northern Hemisphere ice sheets.

7.4. Bolling-Allerod (~15–13 cal ka BP)

A large decrease in $\delta^{18}O$ (~3.0‰) occurs from ~15 to ~13.1 cal ka BP, when sediment deposition switched from gypsum to clay, marking the transition to warmer and/or wetter conditions of the Bolling-Allerod period (Fig. 5). This interval coincides with the main meltwater pulses to the GOM between ~15.2 and 13.0 ka (Flower et al., 2004). At that time, deep-water circulation in the North Atlantic resumed as AMOC intensified (McManus et al., 2004; Liu et al., 2009), the ITCZ migrated north, and precipitation increased in the northern hemisphere Neotropics (Peterson et al., 2000) (Fig. 6). The Petén Itzá record appears to support the model of meltwater routing proposed by Clark et al. (2001), in that input to the GOM led to reduced sea ice, a northward shift of the ITCZ, and increased precipitation in the northern hemisphere Neotropics, whereas diversion to the east into the North Atlantic resulted in reduced AMOC, sea ice expansion, a southward shift in the ITCZ, and drier climate conditions in the northern hemisphere Neotropics.

7.5. Younger Dryas-Preboreal (~13–10.5 cal ka BP)

Higher $\delta^{18}O$ values from ~13.1 to ~11.5 cal ka BP, at least ~4.5‰ greater than modern *L. opesta* $\delta^{18}O$ values, mark the beginning of the Younger Dryas (YD) period (Fig. 5). The onset of the Younger Dryas coincided with a diversion of meltwater from the southern route into the GOM, to an easterly route into the North Atlantic (Broecker et al., 1989), where increased freshwater forcing weakened AMOC and sea ice expanded in the North Atlantic (McManus et al., 2004). During the YD, the Cariaco Basin, off northern Venezuela, experienced colder (~4.5 °C) and drier conditions that have been attributed to a southward shift of the ITCZ (Peterson et al., 2000; Haug et al., 2001; Lea et al., 2003).

Termination of the YD occurred at ~11.5 cal ka BP in Greenland, the Cariaco Basin, and many other geographically distant regions (Haug et al., 2001; NGRIP, 2004). In Petén Itzá, the end of the Younger Dryas is also identified by a modest decrease in $\delta^{18}O$, but not in the magnetic susceptibility record (Fig. 5). A decline in $\delta^{18}O$ starting ~11.5 cal ka BP indicates a change to warmer and/or wetter conditions at the end of the predominantly dry deglacial. Although pollen data also suggest increased rainfall at that time (Bush et al., 2009), gypsum precipitation, which indicates reduced lake volume, continued until the end of the Preboreal period, ~10.0 cal ka BP. The discrepancy between the isotope and lithology data can be reconciled if we accept the idea that lake water levels began to rise around 11.5 cal ka BP, inferred from decreased $\delta^{18}O$, but only attained a sufficient volume to reduce the concentration of calcium and sulfate below gypsum saturation *ca* 10.0 cal ka BP. Oxygen isotope results from the Petén Itzá sediment core are supported by hydrologic proxies from the Cariaco Basin, i.e. increased Ti and Fe concentrations, which show wetter conditions from 11.5 to 10.5 cal ka BP (Haug et al., 2001), presumably as a consequence of a more northerly position of the ITCZ.

7.6. Holocene (~10.5 cal ka BP-present)

During the Pleistocene–Holocene transition, most of the Petén Itzá $\delta^{18}O$ decrease occurred over an extended period between ~10.5 and 7.0 cal ka BP (Curtis et al., 1998), whereas change in Greenland, the North Atlantic and Cariaco was more rapid and occurred before 10.0 cal ka BP (Fig. 7). Slow hydrologic filling of the large, deep Petén Itzá basin may partly explain the protracted period of isotopic change. The pollen record shows that tropical forest, much like the vegetation that characterizes the area today, was established early in the Holocene, indicating sufficient moisture availability to support such a plant community. Dense vegetation during that time period could have promoted high rates of evapotranspiration and soil moisture storage (Rosenmeier et al., 2002), reducing rainwater runoff to the lake. This may account for the slow filling of the basin and protracted period of oxygen isotope equilibration.

Several lines of evidence, however, suggest that regional lakes filled with water rapidly in the early Holocene. First, shallow-water cores from small, deep lakes in the Petén region yielded early

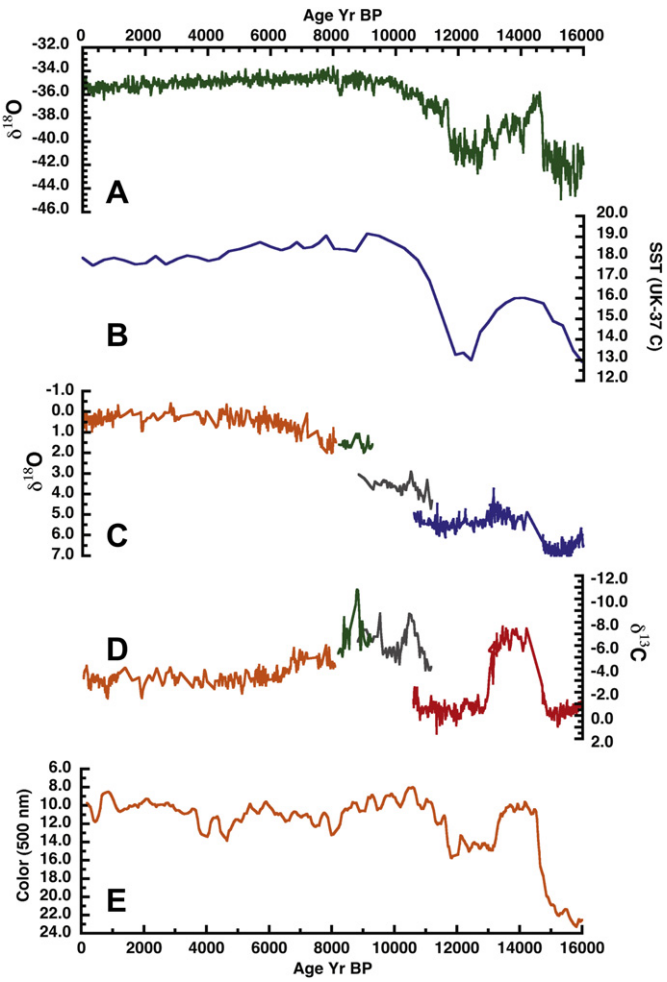

Fig. 7. (A) $\delta^{18}O$ of the NGRIP (North Greenland Ice Core Project members, 2004), (B) sea surface temperatures derived from alkenones in core SU8118 from the subtropical NE Atlantic (Bard et al., 2000), (C) $\delta^{18}O$ of Lake Petén Itzá, (D) $\delta^{13}C$ of Lake Petén Itzá, (E) color reflectance from the Cariaco Basin ODP site 1002 (Peterson et al., 2000). Each record is plotted on its own, independent time scale. (For interpretation of the references to colour in this figure legend, the reader is referred to the web version of this article.)

Holocene basal dates (Deevey, 1978), indicating these shallow-water sites were inundated shortly after the onset of wetter conditions. Second, deep-water cores from small, deep Petén lakes display laminated early Holocene deposits (Deevey et al., 1983), indicating water depths were great enough to enable stable thermal stratification, hypolimnetic anoxia and exclusion of benthic fauna. Third, radiocarbon dates on deep-water (51.6 and 58.2 m) and shallow-water (9.7, 20.9, and 30.0 m) cores from Lake Petén Itzá all show similar dates for the onset of Holocene limnetic sedimentation (11.0–10.2 ^{14}C ka BP), with earliest deep-water Holocene sediments overlying gypsum, and shallow-water deposits overlying paleosols (Hillesheim et al., 2005). If indeed Lake Petén Itzá filled rapidly with the onset of wetter conditions in the early Holocene, it suggests that the decline in δ^{18}O values in the ostracod record between ~7 and 5 cal ka BP, is attributable to a decrease in the isotopic signature of rainfall.

During the glacial and last deglacial periods, δ^{18}O and δ^{13}C fluctuations are positively correlated, whereas in the Holocene, they are negatively correlated. Increased lacustrine productivity during the early Holocene is inferred from higher organic matter content (Curtis et al., 1998) and greater concentrations of *Botryococcus* (Islebe et al., 1996) in a core from the shallow southern basin of Lake Petén Itzá. Algae discriminate against the heavier carbon isotope (^{13}C) in the dissolved inorganic carbon (DIC) of lakewater. The resulting fractionation yields algal biomass that is relatively depleted in ^{13}C and a ^{13}C-enriched DIC pool, the latter leading to relatively high δ^{13}C values in biogenic carbonates.

7.7. Comparison with Southern Hemisphere records

Because of the asynchronous or anti-phase relationship of millennial-scale climate variability between Greenland and

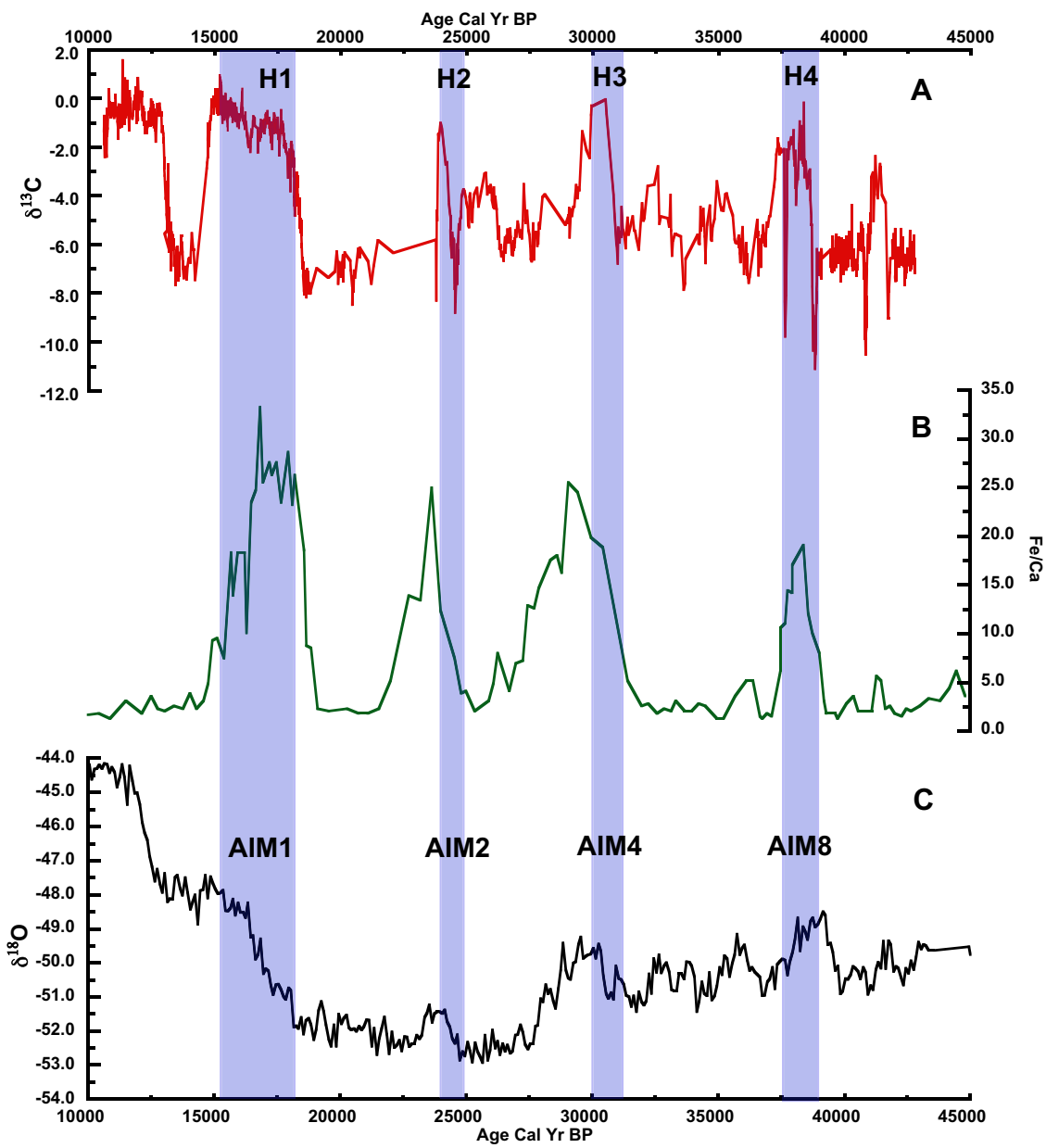

Fig. 8. (A) Carbon isotope data for Lake Petén Itzá, (B) Fe/Ca from Core GeoB 3104-1 off northeastern Brazil (Arz et al., 1998), and (C) δ^{18}O of the EPICA Dronning Maud Land (EDML) Ice Core, Antarctica (EPICA Community Members, 2006). Each record is plotted on its own, independent time scale.

Antarctica during the last Glaciation (EPICA Community Members, 2006), Heinrich stadials and their associated dry periods in Petén are associated with warming in Antarctica during the last glaciation (Hodell et al., 2008). This is supported by the excellent and independent correlation between ostracod $\delta^{13}C$ variations from Petén Itzá and temperature in the Dronning Maud Land area (EDML) ice core record from east Antarctica. Each warming in Antarctica is associated with an increase in $\delta^{13}C$ and inferred drop in Petén Itzá's lake level (Fig. 8). Furthermore, the peaks in $\delta^{13}C$ during Heinrich stadials and Antarctic isotope maxima are anti-phase with wet periods in Brazil inferred from speleothems (Wang et al., 2004) and marine sediment cores off northeastern Brazil (Arz et al., 1998; Jennerjahn et al., 2004; Jaeschke et al., 2007). These observations strongly support an important role for ITCZ migration in affecting precipitation in the Neotropics of both hemispheres during cold stadial periods. Although the movement of the ITCZ has been largely viewed as a response to changes in AMOC and sea ice, we should not exclude the possibility that, instead, tropical climate change may have influenced thermohaline circulation (Guilderson et al., 2001; Seager and Battisti, 2007; Clement and Peterson, 2008).

8. Conclusions

A long sediment core from Lake Petén Itzá, Guatemala, provides a well-dated continental record of climate and environmental variability in the lowland Neotropics that extends into MIS 5A (~85 ka). Stable isotope measurements ($\delta^{18}O$ and $\delta^{13}C$) on ostracod valves in the core yielded a high-resolution record of climate and lake level change spanning the last ~43 ka. Variations in $\delta^{18}O$ and $\delta^{13}C$ are correlated with changes in sediment lithology, suggesting that all three variables responded concurrently to changing climate and limnetic conditions. Gypsum-rich sediments are marked by high $\delta^{18}O$ and $\delta^{13}C$, and were deposited under conditions of high evaporation/precipitation and low lake level. Clay-rich deposits are associated with low $\delta^{18}O$ and $\delta^{13}C$, and represent relatively moister climate conditions and high lake level.

During the glacial period, the average $\delta^{18}O$ value was >3.5‰ greater than mean values in modern ostracod shells, reflecting both colder and drier glacial climate conditions. From 48 to 24 ka, during MIS 3, the thickest gypsum beds and greatest $\delta^{18}O$ and $\delta^{13}C$ values coincide with Heinrich Events 4, 3 and 2. The isotope records support previous interpretations that Heinrich stadials were associated with cold, arid periods in Petén when the ITCZ was displaced southward as a consequence of freshwater input to the North Atlantic, which caused sea ice to expand and AMOC to weaken (Hodell et al., 2008). In contrast, interstadials and the entirety of the Last Glacial Maximum (~24–19 cal ka BP) were marked by clay deposition with lower $\delta^{18}O$ and $\delta^{13}C$ values, reflecting higher lake levels and relatively moister climate.

The pollen, lithological and oxygen isotope data from the Petén Itzá core show that the transition from the LGM to the deglacial involved a shift from cold-wet to cold-dry conditions during HS1. These findings are consistent with paleoclimate reconstructions from western North America and central Mexico (Bradbury, 1997). The isotope results, together with pollen data and independently inferred past water levels, indicate the deglacial period was the time of greatest aridity and lowest lake stage over the last 43 ka. Climate during HS 1 (~19–15 ka) was particularly extreme and the Petén Itzá isotope record contains two $\delta^{18}O$ and $\delta^{13}C$ peaks, with an intervening low. These represent two episodes of cold-arid climate and lake lowstands, separated by a relatively warmer, wetter period and high lake levels at ~17 ka. The isotope maxima coincide with pulses of ice-rafted debris (IRD) recorded off southern Portugal at 17.5 and 16.1 ka (Bard et al., 2000). The Bolling Allerod period marked a transition to clay deposition and low $\delta^{18}O$ and $\delta^{13}C$ values, followed by a return to gypsum precipitation and increased isotopic values at the start of the Younger Dryas. Cold-dry conditions persisted through the Younger Dryas and Preboreal periods, and did not ameliorate until the start of the Holocene, ~10.4 ka (Hillesheim et al., 2005).

The lithologic and stable isotope variations in the Lake Petén Itzá sediment core are linked to known changes in freshwater input to the North Atlantic and Gulf of Mexico. Cold-dry conditions in Petén occurred during times of increased freshwater delivery to the North Atlantic, especially during Heinrich events. When meltwater was diverted south to the Gulf of Mexico during the last deglaciation (e.g., 17 ka and Bolling-Allerod), Petén climate abruptly became more humid. We speculate that alternating routing of fresh water between the North Atlantic and Gulf of Mexico may explain some of the climate transitions observed in Petén Itzá and other North Atlantic records during Termination I. Numerical model experiments suggest that increased flux of fresh water to the North Atlantic decreases the strength of the AMOC, increases sea ice, and causes the ITCZ to shift to a more southerly position. In contrast, meltwater diversion to the Gulf of Mexico has less of an influence on AMOC and almost no effect on North Atlantic sea ice distribution, which has been identified as an important mechanism for ITCZ migration. Our findings appear to support the meltwater routing hypothesis of Clark et al. (2001).

Acknowledgments

We thank the many agencies and individuals in Guatemala who assisted this project. They include: Universidad del Valle, Universidad San Carlos, Ministerio de Ambiente y Recursos Naturales, Consejo Nacional de Areas Protegidas, Instituto de Antropología e Historia, Autoridad Para el Manejo y Desarrollo Sostenible de la Cuenca del Lago Petén-Itzá, Wildlife Conservation Society, Alex Arrivillaga, Cathy Lopez, Margaret Dix, Michael Dix, Margarita Palmieri, David, Rosita, & Kelsey Kuhn, and the staff at La Casa de Don David, Lico Godoy, Tony Ortiz, Franz Sperisen, Luis Toruño, Julian Tesucún, Melisa Orozco, Silja Ramirez, Gabriela Alfaro, and Jacobo Blijdenstein. We also thank the personnel of DOSECC (Drilling, Observation and Sampling of the Earth's Continental Crust) who were instrumental in obtaining the cores. We are indebted to Anders Noren, Kristina Brady and Amy Myrbo of LacCore (National Lacustrine Core Facility), Department of Earth Sciences, University of Minnesota-Twin Cities for their expertise in core acquisition, curation and sampling. This project was funded by grants from the US National Science Foundation, the International Continental Scientific Drilling Program, the Swiss Federal Institute of Technology, and the Swiss National Science Foundation. Radiocarbon analyses were performed under the auspices of the U.S. Department of Energy by Lawrence Livermore National Laboratory under contract DE-AC52-07NA27344. J.E. received support from the School of Natural Resources and Environment, and Land Use and Environmental Change Institute (University of Florida), the Gulf Coast Association of Geological Societies Student Grant Program, the DOSECC Internship for Student Research, and a Geological Society of America Graduate Student Research Grant. D.H. received support from the National Environmental Research Council (NE/I016716/1) of the United Kingdom. L.P and A.S. received support from the Deutsche Forschungsgemeinschaft.

Appendix. Supplementary material

Supplementary material associated with this article can be found, in the online version, at doi:10.1016/j.quascirev.2012.01.020.

References

Anselmetti, F.S., Ariztegui, D., Hodell, D.A., Hillesheim, M.B., Brenner, M., Gilli, A., McKenzie, J.A., Mueller, A.D., 2006. Late Quaternary climate-induced lake level variations in Lake Petén Itzá, Guatemala, inferred from seismic stratigraphic analysis. Palaeogeogr. Palaeoclimatol. Palaeoecol. 230, 52–69.

Arz, H.W., Patzold, J., Wefer, G., 1998. Correlated millennial-scale changes in surface hydrography and terrigenous sediment yield inferred from last-glacial marine deposits off northeastern Brazil. Quat. Res. 50, 157–166.

Baker, P.A., Seltzer, G.O., Fritz, S.C., Dunbar, R.B., Grove, M.J., Tapia, P.M., Cross, S.L., Rowe, H.D., Broda, J.P., 2001. The history of South American tropical precipitation for the past 25,000 years. Science 291, 640–643.

Bard, E., Rostek, F., Turon, J.-L., Gendreau, S., 2000. Hydrological impact of Heinrich events in the subtropical Northeast Atlantic. Science 289, 1321–1324.

Blaauw, M., 2010. Methods and code for 'classical' age-modeling of radiocarbon sequences. Quat. Geochronology 5, 512–518.

Bradbury, J.P., 1997. Sources of glacial moisture in Mesoamerica. Quaternary Int. 43/44, 97–110.

Brady, G.S., 1886. Notes on Entomostraca collected by Mr. A. Haly in Ceylon. J. Linn. Soc. Lond. Zool. 19, 293–317.

Brehm, V., 1939. La fauna microscopica del Lago Peten, Guatemala. An. Esc. Nac. Cienc. Biol. 1, 173–204.

Broecker, W.S., Kennet, J.P., Flower, B.P., Teller, J.T., Trumbore, S., Bonani, G., Wolfli, W., 1989. Routing of meltwater from the Laurentide Ice Sheet during the Younger Dryas cold episode. Nature 341, 318–321.

Bromwich, D.H., Toracinta, E.R., Wei, H., Oglesby, R.J., Fastook, J.L., Hughes, T.J., 2004. Polar MM5 simulations of the winter climate of the Laurentide Ice Sheet at the LGM. J. Clim. 17, 3415–3433.

Bronk-Ramsey, C., 2008. Deposition models for chronological records. Quat. Sci. Rev. 27, 42–60.

Bronk-Ramsey, C., 2001. Development of the radiocarbon calibration program OxCal. Radiocarbon 43, 355–363.

Bush, M.B., Correa-Metrio, A., Hodell, D.A., Brenner, M., Anselmetti, F.S., Ariztegui, D., Mueller, A.D., Curtis, J.H., Grzesik, D., Burton, C., Gilli, A., 2009. Re-evaluation of climate change in lowland Central America during the Last Glacial Maximum using new sediment cores from Lake Petén Itzá, Guatemala. In: Vimeux, F., Sylvestre, F., Khodri, M. (Eds.), Past Climate Variability from the Last Glacial Maximum to the Holocene in South America and Surrounding Regions: Developments in Paleoenvironmental Research. Springer-Verlag, pp. 113–129.

Bush, M.B., De Oliveira, P.E., Colinvaux, P.A., Miller, M.C., Moreno, E., 2004. Amazonian paleoecological histories: one hill, three watersheds. Palaeogeogr. Palaeoclimatol. Palaeoecol. 214, 359–393.

Bush, M.B., Piperno, D.R., Colinvaux, P.A., Krissek, L., De Oliveira, P.E., Miller, M.C., Rowe, W., 1992. A 14,300 year paleoecological profile of a lowland tropical lake in Panama. Ecol. Monogr. 62, 251–276.

Carlson, A.E., Oppo, D.W., Came, R.E., LeGrande, A.N., Keigwin, L.D., Curry, W.B., 2008. Subtropical Atlantic salinity variability and Atlantic meridional circulation during the last deglaciation. Geology 36, 991–994.

Cheng, W., Bitz, C.M., Chiang, J.C.H., 2007. Adjustment of the global climate to an abrupt slowdown of the Atlantic meridional overturning circulation. In: Schmittner, A., Chiang, J.C.H., Hemming, S.R. (Eds.), Past and Future Changes of the Ocean's Meridional Overturning Circulation: Mechanisms and Impacts. AGU Monograph 173. American Geophysical Union, Washington, DC, pp. 295–314.

Chiang, J.C.H., Bitz, C.M., 2005. Influence of high latitude ice cover on the marine Intertropical Convergence Zone. Clim. Dynam. 25, 477–496.

Clark, P.U., Marshall, S.J., Clarke, G.K.C., Hostetler, S.W., Licciardi, J.M., Teller, J.T., 2001. Freshwater forcing of abrupt climate change during the last glaciation. Science 293, 283–287.

Clement, A.C., Peterson, L.C., 2008. Mechanisms of abrupt climate change of the last glacial period. Rev. Geophys. 46, RG4002. doi:10.1029/2006RG000204.

Colinvaux, P.A., Liu, K.B., De Oliveira, P.E., Bush, M.B., Miller, M.C., Steinitz-Kannan, M., 1996. Temperature depression in the lowland tropics in glacial times. Clim. Change 32, 19–33.

Curtis, J.H., Brenner, M., Hodel, D.A., Balser, R.A., Islebe, G.A., Hooghiemstra, H., 1998. A multi-proxy study of Holocene environmental change in the Maya Lowlands of Petén, Guatemala. J. Paleolim. 19, 139–159.

Daday, E., 1905. Untersuchungen uber die Susswasser-Mikrofauna Paraguays. Zoologica 18, 1–374.

Dansgaard, W., 1964. Stable isotopes in precipitation. Tellus 16, 436–468.

Darling, W.G., Bath, A.H., Gibson, J.J., Rozanski, K., 2006. Isotopes in water. In: Leng, M.J. (Ed.), Isotopes in Paleoenvironmental Research. Springer-Verlag, pp. 1–52.

Deevey, E.S., 1978. Holocene forests and Maya disturbance near Quexil Lake, Petén, Guatemala. Pol. Arch. Hydrobiol. 25 (1/2), 117–129.

Deevey, E.S., Stuiver, M., 1964. Distribution of natural isotopes of carbon in Linsley Pond and other New England lakes. Limnol. Oceanogr. 9, 1–11.

Deevey, E.S., Brenner, M., Binford, M.W., 1983. Paleolimnology of the Petén lake district, Guatemala: III. Late Pleistocene and Gamblian environments of the Maya area. Hydrobiologia 103, 211–216.

Enfield, D.B., 1996. Relationships of inter-American rainfall to tropical Atlantic and Pacific SST variability. Geophys. Res. Lett. 23, 3305–3308.

Enfield, D.B., Alfaro, E.J., 1999. The dependence of Caribbean rainfall on the interaction of the tropical Atlantic and Pacific Oceans. J. Clim. 7, 2093–2103.

EPICA Community Members, 2006. One-to-one coupling of glacial climate variability in Greenland and Antarctica. Nature 444, 195–198.

Escobar, J., Curtis, J., Brenner, M., Hodell, D.A., Holmes, J., 2010. Isotope measurement of ostracod and gastropod shells for climate reconstruction: evaluation of within-sample variability and determination of optimum sample size. J. Paleolimnol. 43 (4), 921–938.

Fairbanks, R.G., Mortlock, R.A., Chiu, T.C., Cao, L., Kaplan, A., Guilderson, T.P., Fairbanks, T.W., Bloom, A.L., Grootes, P.M., Nadeau, M.J., 2005. Radiocarbon calibration curve spanning 0 to 50,000 years BP based on paired $^{230}Th/^{234}U/^{238}U$ and ^{14}C dates on pristine corals. Quat. Sci. Rev. 24, 1781–1796.

Flower, B.P., Hastings, D.W., Hill, H.W., Quinn, T.M., 2004. Phasing of deglacial warming and Laurentide Ice Sheet meltwater in the Gulf of Mexico. Geology 32, 597–600.

Ganopolski, A., Rahmstorf, S., 2001. Rapid changes of glacial climate simulated in a coupled climate model. Nature 409, 153–158.

Giannini, A., Kushnir, Y., Cane, M.A., 2000. Interannual variability of Caribbean rainfall, ENSO, and the Atlantic Ocean. J. Clim. 13, 297–311.

Guilderson, T.P., Fairbanks, R.G., Rubenstone, J.L., 2001. Tropical Atlantic coral oxygen isotopes: glacial-interglacial sea surface temperatures and climate change. Mar. Geol. 172, 75–89.

Hastenrath, S., 2002. The Intertropical Convergence Zone of the eastern Pacific revisited. Int. J. Climatol. 22, 347–356.

Hastenrath, S., 1984. Interannual variability and annual cycle: mechanisms of circulation and climate in the tropical Atlantic sector. Mon. Weat. Rev. 112, 1097–1107.

Hastenrath, S., 1978. On modes of tropical circulation and climate anomalies. J. Atmos. Sci. 35, 2222–2231.

Haug, G.H., Hughen, K.A., Sigman, D.M., Peterson, L.C., Röhl, U., 2001. Southward migration of the Intertropical Convergence Zone through the Holocene. Science 293, 1304–1308.

Heaton, T.H.E., Holmes, J.A., Bridgwater, N.D., 1995. Carbon and oxygen isotope variations among lacustrine ostracods: implications for paleoclimatic studies. The Holocene 5, 428–434.

Hemming, S.R., 2004. Heinrich events: massive late Pleistocene detritus layers of the North Atlantic and their global climate imprint. Rev. Geophys. 42, 8755. 1209/04/2003RG000128.

Hillesheim, M.B., Hodell, D.A., Leyden, B.W., Brenner, M., Curtis, J.H., Anselmetti, F.S., Ariztegui, D., Buck, D.G., Guilderson, T.P., Rosenmeier, M.F., Schnurrenberger, D.W., 2005. Lowland neotropical climate change during the late deglacial and early Holocene. J. Quat. Sci. 20, 363–376.

Hodell, D.A., Turchyn, A.V., Wiseman, C.J., Escobar, J., Curtis, J.H., Brenner, M., Gilli, A., Mueller, A.D., Anselmetti, F., Ariztegui, D., Brown, E., 2012. Lateglacial temperature and precipitation changes in the lowland Neotropics by tandem measurement of ?18O in biogenic carbonate and gypsum hydration water. Geochim. Cosmochim. Acta 77, 352–368.

Hodell, D.A., Anselmetti, F.S., Ariztegui, D., Brenner, M., Curtis, J.H., Gilli, A., Grzesik, D.A., Guilderson, T.J., Muller, A.D., Bush, M.B., Correa-Metrio, Y.A., Escobar, J., Kutterolf, S., 2008. An 85-ka record of climate change in lowland Central America. Quat. Sci. Rev. 27, 1152–1165.

Hodell, D.A., Anselmetti, F., Brenner, M., Ariztegui, D., PISDP Scientific Party, 2006. The Lake Petén Itzá scientific drilling project. Scientific Drilling 3, 25–29.

Hooghiemstra, H., Cleef, A.M., Noldus, G.W., Kappelle, M., 1992. Upper Quaternary vegetation dynamics and palaeoclimatology of the La Chonta bog area, Costa Rica. J. Quat. Sci. 7, 205–225.

Hughen, K.A., Overpeck, J.T., Peterson, L.C., Trumbore, S.E., 1996. Rapid climate changes in the tropical Atlantic during the last deglaciation. Nature 380, 51–54.

Islebe, G.A., Hooghiemstra, H., Brenner, M., Curtis, J.H., Hodell, D.A., 1996. A Holocene vegetation history from lowland Guatemala. The Holocene 6, 265–271.

Islebe, G.A., Hooghiemstra, H., van der Borg, K., 1995. A cooling event during the Younger Dryas chron in Costa Rica. Palaeogeogr. Palaeoclimatol. Palaeoecol. 117, 73–80.

Jaeschke, A., Ruehlemann, C., Arz, H., Heil, G., Lohmann, G., 2007. Coupling of millennial-scale changes in sea surface temperature and precipitation off northeastern Brazil with high latitude climate shifts during the last glacial period. Paleoceanography 22, PA4206. doi:10.1029/2006PA001391.

Jennerjahn, T.C., Ittekkot, V., Arz, H.W., Behling, H., Patzold, J., Wefer, G., 2004. Asynchronous terrestrial and marine signals of climate change during Heinrich events. Science 306, 2236–2239.

Jouzel, J., Masson-Delmotte, V., Cattani, O., Dreyfus, G., Falourd, S., Hoffmann, G., Minster, B., Nouet, J., Barnola, J.M., Chappellaz, J., Fischer, H., Gallet, J.C., Johnsen, S., Leuenberger, M., Loulergue, L., Luethi, D., Oerter, H., Parrenin, F., Raisbeck, G., Raynaud, D., Schilt, A., Schwander, J., Selmo, E., Souchez, R., Spahni, R., Stauffer, B., Steffensen, J.P., Stenni, B., Stocker, T.F., Tison, J.L., Werner, M., Wolff, E.W., 2007. Orbital and millennial Antarctic climate variability over the past 800,000 years. Science 317, 793–796.

Kaufmann, A., 1900. Cypriden und Darwinuliden aus der Scweiz. Rev. Suisse Zool. 8, 15–31.

Kim, S.J., Crowley, T.J., Erickson, D.J., Govindasamy, B., Duffy, P.B., Lee, B.Y., 2008. High resolution climate simulation of the Last Glacial Maximum. Clim. Dynam. 31, 1–16.

Knutti, R., Flückiger, J., Stocker, T.F., Timmermann, A., 2004. Strong hemispheric coupling of glacial climate through freshwater discharge and ocean circulation. Nature 430, 851–856.

Kutzbach, J.E., Guetter, P., 1986. The influence of changing orbital parameters and surface boundary conditions on climate simulations for the past 18000 years. J. Atmos. Sci. 43, 1726–1738.

Lachniet, M.S., Patterson, W.P., 2009. Oxygen isotope values of precipitation and surface waters in northern Central America (Belize and Guatemala) are dominated by temperature and amount effects. Earth Planet. Sci. Lett.. doi:10.1016/j.epsl.2009.05.010.

Lea, D.W., Pak, D.K., Peterson, L.C., Hughen, K.A., 2003. Synchroneity of tropical and high latitude Atlantic temperatures over the last glacial termination. Science 301, 1361–1364.

Leng, M.J., Lamb, A.L., Heaton, T.H.E., Marshall, J.D., Wolfe, B.B., Jones, M.D., Holmes, J.A., Arrowsmith, C., 2006. Isotopes in lake sediments. In: Leng, M.J. (Ed.), Isotopes in Paleoenvironmental Research. Elsevier, pp. 147–185.

Leroux, M., 1993. The mobile polar high: a new concept explaining present mechanisms of meridional air-mass and energy exchanges and global propagation of paleoclimatic changes. Glob. Planet. Change 7, 69–93.

Leyden, B.W., Brenner, M., Hodell, D.A., Curtis, J.H., 1994. Orbital and internal forcing of climate on the Yucatan Peninsula for the past ca. 36 ka. Palaeogeogr. Palaeoclimatol. Palaeoecol. 109, 193–210.

Leyden, B.W., Brenner, M., Hodell, D.A., Curtis, J.H., 1993. Late Pleistocene climate in the Central American lowlands. In: Swart, P.K., Lohmann, K.C., McKenzie, J., Savin, S. (Eds.), Climate Change in Continental Isotopic Records. Geophysical Monograph 78. American Geophysical Union, Washington, DC, pp. 165–178.

Liu, Z., Otto-Bliesner, B.L., He, F., Brady, E.C., Tomas, R., Clark, P.U., Carlson, A.E., Lynch-Stieglitz, J., Curry, W., Brook, E., Erickson, D., Jacob, R., Kutzbach, J., Cheng, J., 2009. Transient simulation of last simulation of last deglaciation with a new mechanism for Bolling-Allerod warming. Science 325, 310–314.

McManus, J.F., Francois, R., Gherardi, J.-M., Keigwin, L.D., Brown-Leger, S., 2004. Collapse and rapid resumption of Atlantic meridional circulation linked to deglacial climate changes. Nature 428, 834–837.

Mix, A.C., Bard, E., Schneider, R., 2001. Environmental processes of the ice age: land, oceans, glaciers (EPILOG). Quat. Sci. Rev. 20, 627–657.

Mueller, A.D., Islebe, G., Hillesheim, M.B., Grzesik, D., Anselmetti, F.S., Ariztegui, D., Brenner, M., Curtis, J.H., Hodell, D.A., McKenzie, J.A., Venz-Curtis, K., 2009. Climate drying and associated forest decline in the lowlands of northern Guatemala during the late Holocene. Quat. Res. 71, 133–141.

Mueller, A.D., Anselmetti, F.S., Ariztegui, D., Brenner, M., Curtis, J.H., Escobar, J., Gilli, A., Grzesik, D.A., Hodell, D.A., Guilderson, T.J., Kutterolf, S., Ploetze, M.L., 2010. Late Quaternary Palaeoenvironment of Lake Petén Itzá, northern Guatemala: evidence from deep drill holes and seismic stratigraphy. Sedimentology 57, 1220–1245.

North Greenland Ice Core Project members, 2004. High-resolution record of Northern Hemisphere climate extending into the Last Interglacial period. Nature 431, 147–151.

Oana, S., Deevey, E.S., 1960. Carbon 13 in lake waters, and its possible bearing on paleolimnology. Am. J. Sci. 258-A, 253–272.

Otto-Bliesner, B.L., Brady, E.C., 2010. The sensitivity of the climate response to the magnitude and location of freshwater forcing: Last Glacial Maximum experiments. Quat. Sci. Rev. 29, 56–73.

Peterson, L.C., Haug, G.H., Hughen, K.A., Röhl, U., 2000. Rapid changes in the hydrologic cycle of the tropical Atlantic during the Last Glacial. Science 290, 1947–1951.

Pérez, L., Lorenschat, J., Bugja, R., Brenner, M., Scharf, B., Scwalb, A., 2010. Distribution, diversity and ecology of modern freshwater ostracodes (Crustacea), and hydrochemical characteristics of Lago Petén Itzá, Guatemala. J. Limnol. 69, 146–159.

Pérez, L., Frenzel, P., Brenner, M., Escobar, J., Hoelzmann, P., Scharf, B., Schwalb, A., 2011. Late Quaternary (24–10 ka BP) environmental history of the Neotropical lowlands inferred from ostracodes in sediments of Lago Petén Itzá, Guatemala. J. Paleolimnol. 46, 59–74.

Piperno, D.R., Bush, M.B., Colinvaux, P.A., 1990. Paleoenvironments and human occupation in late-Glacial Panama. Quat. Res. 33, 108–116.

Portig, W.H., 1965. Central American rainfall. Geographical Rev. 55, 68–90.

Poveda, G., Waylen, P.R., Pulwarty, R.S., 2006. Annual and inter-annual variability of the present climate in northern South America and southern Mesoamerica. Palaeogeogr. Palaeoclimatol. Palaeoecol. 234, 3–27.

Rasmussen, S.O., Andersen, K.K., Svensson, A.M., Steffensen, J.P., Vinther, B.M., Clausen, H.B., Siggaard-Andersen, M.L., Johnsen, S.J., Larsen, L.B., Dahl-Jensen, D., Bigler, M., Rothlisberger, R., Fischer, H., Goto-Azuma, K., Hansson, M.E., Ruth, U., 2006. A new Greenland ice core chronology for the last glacial termination. J. Geophys. Res.. doi:10.1029/2005JD006079.

Reimer, P.J., Baillie, M.G.L., Bard, E., Bayliss, A., Beck, J.W., Blackwell, P.G., Bronk Ramsey, C., Buck, C.E., Burr, G.S., Edwards, R.L., Friedrich, M., Grootes, P.M., Guilderson, T.P., Hajdas, I., Heaton, T.J., Hogg, A.G., Hughen, K.A., Kaiser, K.F., Kromer, B., McCormac, F.G., Manning, S.W., Reimer, R.W., Richards, D.A., Southon, J.R., Talamo, S., Turney, C.S.M., van der Plicht, J., Weyhenmeyer, C.E., 2009. INTCAL09 and MARINE09 radiocarbon age calibration curves, 0–50,000 years Cal BP. Radiocarbon 51, 1111–1151.

Rind, D., Rossow, W.B., 1984. The effects of physical processes on Hadley circulation. J. Atmos. Sci. 41, 479–507.

Roche, D.M., Wiersma, A.P., Renssen, H., 2010. A systematic study of the impact of freshwater pulses with respect to different geographical locations. Clim. Dynam. 34, 997–1013.

Rosenmeier, M.F., Hodell, D.A., Brenner, M., Curtis, J.H., Martin, J.B., Anselmetti, F.S., Ariztegui, D., Guilderson, T.P., 2002. Influence of vegetation change on watershed hydrology: implications for paleoclimatic interpretation of lacustrine $\delta^{18}O$ records. J. Paleolimnol. 27, 117–131.

Seager, R., Battisti, D., 2007. Challenges to our understanding of the general circulation: abrupt climate change. In: Schneider, T., Sobel, A.H. (Eds.), The Global Circulation of the Atmosphere. Princeton Univ. Press, Princeton, N. J., pp. 331–371.

Spencer, H., Slingo, J., Davey, M., 2004. Seasonal predictability of ENSO teleconnections: the role of the remote ocean response. Clim. Dynam. 22, 511–526.

Stager, J.C., Ryves, D.B., Chase, B.M., Pausata, F.S.R., 2011. Catastrophic drought in the Afro-Asian monsoon region during Heinrich event 1. Science. doi:10.1126/science.1198322.

Stuiver, M., Polach, H.A., 1977. Discussion: reporting of 14C data. Radiocarbon 19, 355–363.

Taylor, M.A., Enfield, D.B., Chen, A.A., 2002. Influence of the tropical Atlantic versus the tropical Pacific on Caribbean rainfall. J. Geophys. Res. 107. doi:10.1029/2001JC001097.

Wang, C., Enfield, D.B., Lee, S.K., Landsea, C.W., 2006. Influences of the Atlantic warm pool on western hemisphere summer rainfall and Atlantic hurricanes. J. Clim. 19, 3011–3028.

Wang, X., Auler, A.S., Edwards, R.L., Cheng, H., Cristalli, P.S., Smart, P.L., Richards, D.A., Chuan-Chou, S., 2004. Wet periods in northeastern Brazil over the past 210 kyr linked to distant climate anomalies. Nature 432, 740–743.

Williams, C., Flower, B.P., Hastings, D.W., Guilderson, T.P., Quinn, K.A., Goddard, E.A., 2010. Deglacial abrupt climate change in the Atlantic warm pool: a Gulf of Mexico perspective. Paleoceanography 25, PA4221. doi:10.1029/2010PA001928.

Yurco, L.N., 2010. A Multi-Proxy Investigation of the Late Glacial "Mystery Interval" (17.5–14.5 ka) in Cariaco Basin. M.S. Thesis, University of Miami, United States.